A BAG3 Coding Variant in Mice Determines Susceptibility to Ischemic Limb Muscle Myopathy by Directing Autophagy

Joseph M. McClung, PhD[1,2], **Timothy J. McCord, BS**[3], **Terence E. Ryan, PhD**[1,2], **Cameron A. Schmidt, BS**[1,2], **Thomas D. Green, BS**[1,2], **Kevin W. Southerland, MD**[4], **Jessica L. Reinardy, PhD**[3,5], **Sarah B. Mueller, PhD**[3,5], **Talaignair N. Venkatraman, PhD**[6], **Christopher D. Lascola, MD, PhD**[6], **Sehoon Keum, PhD**[7], **Douglas A. Marchuk, PhD**[7], **Espen E. Spangenburg, PhD**[1,2], **Ayotunde Dokun, MD**[8,10], **Brian H. Annex, MD**[8,9,10], and **Christopher D. Kontos, MD**[3,5]

[1]Department of Physiology, East Carolina University, Brody School of Medicine, Greenville, NC

[2]Diabetes and Obesity Institute, East Carolina University, Brody School of Medicine, Greenville, NC

[3]Department of Medicine, Division of Cardiology, Duke University Medical Center, Durham, NC

[4]Department of Surgery, Division of General Surgery, Duke University Medical Center, Durham, NC

[5]Department of Pharmacology and Cancer Biology, Duke University Medical Center, Durham, NC

[6]Department of Radiology, Duke University Medical Center, Durham, NC

[7]Department of Molecular Genetics and Microbiology, Duke University Medical Center, Durham, NC

[8]Department of Medicine, Division of Endocrinology, University of Virginia School of Medicine, Charlottesville, VA

[9]Division of Cardiovascular Medicine, University of Virginia School of Medicine, Charlottesville, VA

[10]The Robert M. Berne Cardiovascular Research Center, University of Virginia School of Medicine, Charlottesville, VA

Abstract

Background—Critical limb ischemia (CLI) is a manifestation of peripheral artery disease (PAD) that carries significant mortality and morbidity risk in humans, although its genetic determinants remain largely unknown. We previously discovered two overlapping quantitative trait loci (QTL) in mice, *Lsq-1* and *Civq-1*, that affected limb muscle survival and stroke volume following

---

femoral artery or middle cerebral artery ligation, respectively. Here we report that a *Bag3* variant (Ile81Met) segregates with tissue protection from hindlimb ischemia (HLI).

Methods—We treated mice with either adeno-associated viruses (AAV) encoding a control (GFP), or two BAG3 variants, namely Met81 or Ile81, and subjected the mice to hindlimb ischemia.

Results—We found that the BAG3 Ile81Met variant in the C57BL/6 (BL6) mouse background segregates with protection from tissue necrosis in a shorter congenic fragment of *Lsq-1 (*C.B6-*Lsq1-3*). Treating BALB/c mice with AAV encoding the BL6 BAG3 variant (Ile81) (n=25) displayed reduced limb tissue necrosis and increased limb tissue perfusion compared to Met81- (n=25) or GFP- (n=29) expressing animals. BAG3^{Ile81}, but not BAG3^{Met81}, improved ischemic muscle myopathy and muscle precursor cell differentiation and improved muscle regeneration in a separate, toxin-induced model of injury. Systemic injection of AAV-BAG3^{Ile81} (n=9), but not BAG3^{Met81} (n=10) or GFP (n=5), improved ischemic limb blood flow, limb muscle histology, and restored muscle function (force production). Compared to BAG3^{Met81}, BAG3^{Ile81} displayed improved binding to the small heat shock protein (HspB8) in ischemic skeletal muscle cells and enhanced ischemic muscle autophagic flux.

Conclusions—Taken together, our data demonstrate that genetic variation in BAG3 plays an important role in the prevention of ischemic tissue necrosis. These results highlight a pathway that preserves tissue survival and muscle function in the setting of ischemia.

Although progress has been made in elucidating the contribution of genetic factors to the development of peripheral artery disease (PAD) [1–6], no alleles that modulate patients' susceptibility to critical limb ischemia (CLI) are presently known. Historically, it was felt that CLI represented the natural progression of PAD in patients with intermittent claudication. However, differences in the clinical course of CLI raise the intriguing possibility that CLI represents a distinct phenotypic manifestation of PAD that is dependent on genetic determinants of the susceptibility to limb necrosis [3, 7–12]. Identifying the genes/ proteins that either contribute to or protect against patients' susceptibility to CLI will be critical to develop therapies that promote limb salvage. Accordingly, genetic analysis in inbred mouse strains identified a 37-gene quantitative trait locus (QTL) on chromosome 7 termed *Lsq-1*, which was associated with tissue survival and perfusion recovery following hind limb ischemia (HLI) induced by femoral artery ligation [8, 9, 12, 13]. To date, 2 genes within this QTL (*ADAM12* and *IL-21R*) have been found to play at least a partial role in the differential perfusion recovery observed among C57BL/6 (BL6), BALB/c, and other inbred strains of mice following HLI [14, 15].

A notable feature of *Lsq-1* is its association not only with perfusion recovery but also with muscle necrosis [8], raising the possibility that genes related to myogenesis and muscle function might be relevant to ischemic tissue survival, as we have suggested previously [16]. Muscle function is an accurate predictor of morbidity/mortality outcomes in PAD[17–19], thus

the ability of muscle to regenerate and generate force after ischemic injury could be a critical determinant of clinical outcomes. With this in mind, we investigated effects of genetic variants in a candidate gene within *Lsq-1*, Bcl-2-associated athanogene-3 (*Bag3*), that has an established role in skeletal muscle cell biology [20–22]. BAG3 is required for myofibrillar integrity through its interactions with HSP70 and CAPZ [23]; variants in BAG3 have been causally linked to myofibrillar myopathy [22] and dilated cardiomyopathy in humans [24, 25]; and loss of BAG3 in mice causes perinatal lethality due to fulminant skeletal myopathy [26].

An additional function of BAG3 that supports a potential critical role in regulating the tissue response to ischemia is its ability to regulate autophagy [27–31], the process by which defective cellular components are degraded and recycled to ensure proper cellular function [32]. Autophagic removal of damaged proteins is required for the maintenance of normal skeletal muscle homeostasis, as transgenic mice with muscle-specific defects in autophagy develop progressive myopathy and abnormal muscle metabolism [33, 34]. Despite recent research related to autophagy's role in the ischemic brain[35] and heart (reviewed in [36]), very little is known about the role of autophagy or its mechanisms of regulation in ischemic skeletal muscle. A link between BAG3's regulation of autophagy and ischemic muscle injury has not been established, although identifying such a connection could provide a unique cellular target to influence tissue regeneration and blood flow through the efficient processing of cellular aggregates after ischemic injury.

Here, using adeno-associated virus (AAV)-mediated expression of BAG3 variants in BL6 and BALB/c mice in a model of limb ischemia, in a model of toxin-induced muscle regeneration, and in muscle cell-specific experiments *in vitro*, we report a coding variant in *Bag3* that contributes significantly to ischemic muscle necrosis after HLI. We show that tissue necrosis, limb perfusion and vascular density, defective ischemic muscle regeneration, and limb muscle contractile function can all be rescued by a single BL6 coding variant in *Bag3* (Ile81) that functions, at least in part, through the regulation of ischemic myofiber regeneration and cellular autophagy.

Materials and Methods

(Detailed methodology can be found in the online data supplement)

Animals

Experiments were conducted on adult C57/BL6J (*n*=34), BALB/cJ (*n*=151), or BALB/c congenic mice containing a 12.06 Mb region of chromosome 7 from C57/BL6J (C.B6-*Lsq1*-3 or also known as C.B6-*Civq1-3*[37] Congenic; *n*=5) (all ≤10 weeks old), were approved by the East Carolina University, Duke University, or University of Virginia Institutional Animal Care and Use Committees, and conformed to the Guide for the Care and Use of Laboratory Animals published by the US National Institutes of Health. Hindlimb ischemia (HLI), necrosis monitoring, and laser Doppler perfusion monitoring were performed as described previously[8]. The cardiotoxin model of mouse muscle regeneration was performed as described previously using intramuscular injections of *Naja nigricollis* venom[38]. After systemic adeno-associated virus (AAV) injection, HLI surgeries were

modified by leaving the inferior epigastric, lateral circumflex, and superficial epigastric artery collateral branches intact.

MRI

MR imaging was performed on a Bruker 7T (70/30) system (Bruker Biospin, Billerica, MA, USA). ADC perfusion imaging and magnetic resonance angiography (MRA) for assessment of collateralization were performed with ABLAVAR (Lantheus Medical Imaging, Inc.), a novel blood pool agent, to image vascular volume and collateral vessels.

Cell Lines and Culture

Murine C2C12 and C3H-10T1/2 cell lines were purchased from ATCC. Immortalized EC-RF24 cells (ECRF)[39] were a gift from Dr. Hans Pannekoek, The University of Amsterdam. Human umbilical vein endothelial cells (HUVECs) were isolated from donor placental umbilical veins and used prior to passage 6. GP2-293 and 293 cells for adenovirus generation were cultured in DMEM with 10% FBS. Primary murine skeletal myoblasts were isolated as described[40].

Limb Muscle Morphology and Regeneration

Histological staining and immunofluorescence was performed according to standard procedures on 8-μm-thick transverse sections of tibialis anterior (TA) muscle. Contractile force measurements were performed using single extensor digitorum longus (EDL) muscles, as described previously [41].

Virus Generation

Pantrophic *BAG3* shRNA or *GFP* control retroviruses were generated by cotransfection of GP2-293 cells with shRNA (SABiosciences) and envelope (VSVG) plasmids. Adenoviruses were generated by transfection of Adeno-X 293 cells using CalPhos Mammalian Transfection Kit (Clontech). Adeno-Associated Viruses (GFP, BAG3[Met81], BAG3[Ile81]) were generated and purified by column chromatography at the UNC Viral Vector Core Facility.

Autophagic Flux

Autophagic flux was assessed in myotubes using an adenovirus expressing the RFP-GFP-LC3 reporter[42]. Punctate structures with GFP-RFP and/or RFP signals were quantified in more than 120 cells per group, and the degree of autophagosome maturation was expressed as the percent of puncta with red color, as previously described[43].

Statistical Analysis

Statistical analyses were carried out using StatPlus:mac (v. 2009) statistical analysis software, Vassarstats (www.vassarstats.net), or Prism 6 (v. 6.0d). Non-parametric necrosis score and peak specific force (% Control) data were compared using Kruskal-Wallis tests and Mann-Whitney U Tests, where appropriate, for post-hoc analyses. For MR angiography analyses, data were evaluated using Student's *t*-test. Correlation data for BAG3 protein and muscle force production were performed using least squares regression procedure. Data corrected for control limbs were analyzed using paired t-tests. All other data were compared

using ANOVA or repeated measures ANOVA with Tukey's post hoc tests or Student's 2-tailed *t*-test. In all cases, $P < 0.05$ was considered statistically significant and values are presented as means ± SE.

Results

Identification of Bag3 as a potential protective gene in ischemic tissue necrosis

C57BL/6×BALB/c offspring were bred to parental BALB/c mice to generate a line of BALB/c mice (C.B6-*Lsq1-3*) congenic for a ~12.06 Mb region of BL6 chr. 7 (Congenic) that includes *Bag3* but excludes 19 other genes from *Lsq-1* (Supplementary Figure 1). This line is the same as the previously reported C.B6-*Civq1-3*[37] Congenic. These mice were subjected to HLI alongside parental BL6 and BALB/c mice, and necrosis scores were determined 7 days later (Figure 1A). The degree of tissue necrosis in Congenic mice mirrored that of parental BL6 mice, indicating that BL6-encoded variants in this region contributed to muscle survival. Histological analysis of ischemic limb muscle largely revealed a restoration of ischemic muscle (L) fascicular and vascular morphology compared to the contralateral limb (R) (Figure 1B), which we have previously observed in BL6 but not BALB/c mice[44–46]. Myofiber integrity (non-myofiber area), regeneration (embryonic MyHC$^+$), and capillary density (CD31$^+$) were all similar in the ischemic limbs of Congenic and BL6 mice but were significantly different from those in BALB/c mice (Figure 1C–E). *Bag3* mRNA expression was significantly greater in BL6 mice on day 1 after HLI (Figure 1F), a time when limb perfusion is comparable between the strains [8]. Together these data support the possibility that BAG3, as a member of *Lsq-1*, plays a role in ischemic muscle survival.

BAG3^{Ile81} gain of function induces BALB/c muscle hypertrophy and vascular expansion

Sequencing of the coding region and known regulatory elements of *Bag3* revealed an isoleucine to methionine change at residue 81 (I81M), a position with little conservation among a number of mammalian species despite a high degree of similarity of surrounding residues (Supplementary Figure 2). To test whether either variant would alter the basal muscle morphology or vascular profile, we injected serotype 6 adeno-associated viruses (AAV6) encoding either variant of BAG3 with a FLAG epitope tag into both the TA and gastrocnemius (Gastroc) muscles of BALB/c mice. AAV6-BAG3 expression was verified *in vivo* by immunofluorescence (IF) microscopy for FLAG (Supplementary Figure 3. In BALB/c muscles, mRNA (Figure 2A) and protein (Figure 2B) of the two variants were expressed at equal levels in non-ischemic muscle. The BL6 variant (BAG3^{Ile81}) slightly but significantly increased TA myofiber size (Figure 2C, D) andmuscle CD31$^+$ vessel density (Figure 2E, F). Despite these vascular changes, LDPI-measured perfusion was not affected by either variant at baseline (Figure 2G, H).

The BL6 BAG3 variant, BAG3^{Ile81}, prevents ischemic limb necrosis in BALB/c mice

We next asked whether the BL6 variant, BAG3^{Ile81}, could protect against ischemic necrosis in BALB/c mice. We first confirmed that the two variants were expressed at equal levels after HLI (Supplementary Figure 4). Notably, injection of either variant rescued the ischemia-induced loss of BAG3 protein and *Bag3* mRNA but did not result in significant

overexpression compared to baseline. Strikingly, expression of BAG3[Ile81] in BALB/c mice conferred significant protection against ischemic tissue necrosis (Figure 3A). We verified similar perfusion deficits immediately post HLI surgery using LDPI (Supplementary Figure 5), but because the susceptibility to ischemic tissue necrosis has been linked to tissue perfusion [8, 11–13, 47, 48], we used magnetic resonance angiography (MRA) to examine limb muscle perfusion. Expression of BAG3[Ile81], but not BAG3[Met81], significantly increased vascular volume and apparent diffusion coefficient (ADC) perfusion (Figure 3B, C) in the ischemic limb. To assess the vascular effects of BAG3[Ile81], we performed IF for vascular markers (Figure 3D). On day 7 post-HLI, CD31^{+} capillary density decreased significantly in BALB/c mice expressing GFP or BAG3[Met81] compared to BL6, whereas BAG3[Ile81] expression rescued CD31^{+} density to levels that were similar to the ischemic BL6 (Figure 3E). Importantly, expression of BAG3[Ile81] in BALB/c mice conferred protection against necrosis up to 21 days after HLI (Figure 3F).

BAG3[Ile81] promotes muscle regeneration by enhancing myofiber differentiation and muscle precursor cell fusion

Bag3 null mice[40] and humans with certain BAG3 mutations[22, 49, 50] undergo marked skeletal muscle degeneration with a failed regenerative response. This phenotype is similar to that observed in ischemic BALB/c mice, suggesting that the BAG3 variants might differentially regulate muscle regeneration. Ischemic limb muscle from BAG3[Ile81]-expressing BALB/c mice appeared morphologically similar to that in BL6 mice (Figure 4A) and quantitatively displayed similar non-myofiber area (Figure 4B) and intact myofiber cross-sectional area (Figure 4C), consistent with either protection from ischemic injury or an improved regenerative response. To test this, we quantified myofiber regeneration after AAV delivery and HLI. The number of eMyHC[+] myofibers was reduced in GFP- and BAG3[Met81]-expressing mice compared to BL6 mice, and expression of BAG3[Ile81] partially rescued this deficit (Figure 4D–E). GFP or BAG3[Met81] myofibers expressing eMyHC[+] were also smaller than those expressing BAG3[Ile81] (Figure 4F). To determine whether *Bag3* variation has a general impact on BALB/c skeletal muscle regeneration, we tested the BAG3 variants' effects following *Naja nigricolis* venom injection, a commonly used model of skeletal muscle regeneration [38]. Similar to our results in the HLI model, resolution of muscle injury was accelerated in BALB/c mice expressing BAG3[Ile81] compared to GFP or BAG3[Met81] (Supplementary Figure 6), as demonstrated by a significant reduction in non-contractile tissue and greater myofiber size. Taken together, these results suggest that the BAG3[Ile81] variant promotes muscle regeneration in different models of muscle injury, and it confers dominant protection in BALB/c mice, which endogenously express BAG3[Met81].

Muscle regeneration depends on the number, function, and proliferation of PAX7^{+} satellite cells. Compared to non-ischemic BALB/c muscle, PAX7^{+} nuclei increased in all groups after HLI, and no significant differences were noted among BAG3 variants (Supplementary Figure 7A–B), indicating that HLI induces the PAX7^{+} muscle cell proliferative response independent of the BAG3 variant. These findings were confirmed *in vitro* in C2C12 (SFigure 7C) and primary BALB/c myoblasts (Supplementary Figure 7D), in which expression of either BAG3 variant or GFP had no effect on skeletal myoblast proliferation. Stable silencing of BAG3 expression in C2C12 myoblasts using retroviral shRNA resulted in a

slight but significant decrease in cell number after 72 and 96 hours of proliferation (Supplementary Figure 7E), however this effect was due to increased cell death (not shown), which has been demonstrated previously[20].

Muscle regeneration also depends on precursor cell differentiation and fusion with existing myofibers. BAG3[Ile81] expression restored the mRNA expression of the myogenic regulatory factor myogenin (Figure 4G) and the differentiation/fusion proponent Tmem8c (myomaker; Figure 4H) to BL6 levels during ischemia, consistent with improved differentiation and fusion capacity. *In vitro*, the fusion of BALB/c primary myoblasts into myotubes was significantly increased by BAG3[Ile81] (Figure 4I, J). Furthermore, myotube formation by C2C12 myoblasts co-cultured with a predominance of 10T1/2 pluripotent pericytes was improved by BAG3[Ile81] (Figure 4K). Taken together, these results demonstrate that BAG3[Ile81] promotes ischemic muscle regeneration in part by enhancing muscle precursor cell differentiation and fusion.

BAG3[Met81] expression in ischemic BL6 mice does not act as a dominant negative inhibitor

Previous genetic studies showed that a single copy of the BAG3[Ile81] variant, e.g., in first generation offspring of BL6×BALB/c crosses, has a dominant protective effect on ischemic muscle survival [8]. To verify this effect, we investigated whether expression of the BALB/c variant, BAG3[Met81], in BL6 mice would affect the response to ischemia. BL6 mice were injected IM with AAV encoding BAG3[Met81] then subjected to HLI, and no adverse effects on tissue survival were observed. Histological and IF analyses revealed no alterations in muscle morphology, PAX7^{+} cell number, eMyHC expression, regenerating myofiber size, or CD31^{+} vessel density when compared to uninfected BL6 mice 7 days after HLI (Figure 5A–F).

Systemic BAG3[Ile81] delivery rescues limb blood flow and force production in the ischemic BALB/c limb

We next sought to determine whether BAG3[Ile81]-mediated muscle regeneration in BALB/c mice resulted in functional muscle improvements (i.e., isometric muscle force production) as measured *ex vivo* in EDL muscles. Because of the substantial necrosis observed in control BALB/c mice, we made two modifications to our approach. First, we took advantage of the tropism of AAV6 for muscle to deliver AAVs encoding GFP or BAG3 systemically (by IV injection) to effect expression in all muscle groups of the hindlimb, including the extensor digitorum longus (EDL) muscle. Second, we refined the HLI model to limit muscle necrosis by leaving all major collateral vessels intact, which induces less severe limb ischemia [40]. Rescue of ischemic *Bag3* mRNA expression was verified by qRT-PCR (Figure 6A). The modified ischemic injury resulted in mild necrosis only in the GFP- and BAG3[Met81]-expressing mice (Figure 6B). Blood flow recovery was significantly less in GFP- and BAG3[Met81]-treated BALB/c mice, but BAG3[Ile81] expression returned perfusion recovery to BL6 levels (Figure 6C–D). Force production in non-ischemic control EDL muscle was not different in any treatment group (Figure 6E). Although force production was significantly impaired in all ischemic BALB/c EDL muscles, BAG3[Ile81] expression rescued force production across a range of frequencies (Figure 6F) and improved peak specific force (Figure 6G) compared to GFP- and BAG3[Met81]-expressing mice. Correlational analysis

revealed a strong positive association between BAG3[Ile81] expression and limb muscle peak specific force (N/cm^2) in BALB/c muscle (Figure 6H). Muscle histology, qualitatively assessed by H&E, demonstrated intact fascicular arrangements and centralized myofiber nuclei in muscles from BAG3[Ile81]-expressing mice and degenerative, anucleate myofibers in GFP- and BAG3[Met81]-expressing ischemic limb muscles (Figure 6I), similar to the histological changes observed with IM injection of BAG3[Ile81].

Autophagy is differentially regulated in ischemic BALB/c and BL6 muscle and by BAG3 variants

Autophagy is a critical biological process regulating myopathic regeneration in skeletal muscle cells[34, 51–53] and is believed to partially drive endothelial cell tube formation *in vitro*[54], but its role in the differential susceptibility to ischemic myopathy between mouse strains is unknown. To investigate this role, we analyzed skeletal muscle from the ischemic limbs of BL6 and BALB/c mice during the initial week of hindlimb ischemia. Transcriptional analysis demonstrated an increase in LC3 mRNA expression in both BL6 and BALB/c limb muscles 3 days after limb ischemia, which returned to baseline 7 days after HLI only in BL6 mice (Figure 7A). Other autophagy-related transcripts (ULK1, ATG7, Gabarap, SQSTM1, and CTSL) were similarly induced early after ischemia (HLI d3) in both BL6 and BALB/c limb muscles and decreased 7 days after HLI only in BL6 limb muscles (Supplementary Figure 8A). LC3II protein abundance, a product of lipidation, paralleled ischemic mRNA expression at HLI d7 in BL6 and BALB/c mice (Figure 7B, C). In order to understand whether the BAG3 variants differentially affect autophagy *in vivo*, qRT-PCR was performed on muscle samples from BALB/c mice injected retro-orbitally with AAV-BAG3 variants. BAG3[Ile81], but not GFP- or BAG3[Met81], reduced LC3 mRNA in BALB/c limb muscle 7 days after HLI (Figure 7D). However, BAG3[Ile81] did not alter the expression of other autophagy-related transcripts *in vivo* (Supplementary Figure 8B). LC3II protein abundance 7 days after HLI paralleled the ischemic LC3 mRNA expression in AAV-treated BALB/c mice (Figure 7E, F). Collectively, these data provide direct evidence that autophagy progresses differentially in ischemic BL6 and BALB/c limb muscle and that exogenous expression of BAG3[Ile81] in BALB/c mice recapitulates the phenotype observed in BL6 mice.

BAG3[Ile81] differentially binds a small heat shock protein (HspB8) and regulates ischemic muscle cell autophagic flux

The variant amino acid residue 81 flanks the first IPV domain in BAG3[29], a domain that is known to play a role in directing autophagy[55]. Therefore, we next specifically examined the effect of the BAG3 variants on the expression and interaction of proteins linked to autophagic flux. Using limb skeletal muscles early after HLI (days 1 and 3), we assessed Hsp70, HspB8, and SQSTM1 (p62) protein abundances in BL6 and BALB/c limb muscles. HspB8 demonstrated more persistent expression after ischemia in BL6 muscle compared to BALB/c muscle (Supplementary Figure 9). To examine the effects of the BAG3 variants on the interaction with these proteins after ischemia, we infected BALB/c primary muscle cells *in vitro* with AAVs encoding GFP, BAG3[Met81], and BAG3[Ile81], subjected them to experimental ischemia, and blotted whole cell lysates for HspB8 and SQSTM1 (Figure 8A; Supplementary Figure 10A). The expression of SQSTM1 was not affected by either BAG3 variant, however HspB8 protein was increased by BAG3[Ile81]. Similarly,

immunoprecipitation of FLAG-tagged BAG3 constructs from these lysates (Figure 8B; Supplementary Figure 10B) revealed greater binding of HspB8 to BAG3^{Ile81}. We next examined effects of the BAG3 variants on autophagic flux in BALB/c muscle progenitor cells and myotubes [28]. To test this, we co-infected primary BALB/c myoblasts with viruses expressing either BAG3 variant and an RFP-GFP-LC3 reporter[42]. The expression of BAG3^{Ile81}, but not BAG3^{Met81}, rescued autolysosome formation in ischemic BALB/c muscle myoblasts (Figure 8C) and differentiated myotubes (Figure 8D) to the level observed in BL6 myoblasts and myotubes, respectively. These results indicate that BAG3^{Ile81} expression in both undifferentiated myoblasts and differentiated myotubes rescues an inherent BALB/c muscle cell impairment in autophagic flux that is paralleled by enhanced binding to HspB8.

Discussion

In this study we found that a single coding polymorphism in a gene within the *Lsq-1* QTL, *Bag3*, partially determines susceptibility to skeletal muscle tissue necrosis following HLI in mice. An isoleucine to methionine variant at position 81 in the murine BAG3 protein was sufficient to confer susceptibility to necrosis in BALB/c mice. In contrast, the BL6 variant (Ile81) conferred a protective effect that could rescue ischemic BALB/c myopathy as well as limb muscle perfusion. Importantly, re-expression of the BAG3^{Met81} variant was not sufficient to rescue necrosis or restore limb muscle integrity or vascular density, suggesting a functional difference in the two BAG3 variants related to myogenesis and possibly neovascularization. Importantly, additional studies revealed a differential effect of the two variants on ischemic skeletal muscle cell autophagy, with BAG3^{Ile81} promoting autophagic flux. The susceptibility of BALB/c and other inbred mouse strains to ischemic muscle tissue injury has been used as a model of human critical limb ischemia, and as such, elucidating the genetic mechanisms responsible for the widely divergent responses observed among different strains may provide critical insights into the treatment and/or prevention of CLI in patients.

The current findings support previous studies demonstrating that the presence of at least one copy of BL6 Chr. 7, which contains *Bag3*, is sufficient to confer protection from ischemic injury in both the hind limb and the brain [8, 12]. Accordingly, in our study BALB/c mice congenic for a fragment of the BL6 *Lsq-1* QTL that contained the BL6 variant of *Bag3* were resistant to ischemic tissue necrosis, displaying enhanced myofiber integrity and regeneration after HLI as well as increased vascular density. Although many other genes with a variety of known and putative functions are contained within *Lsq-1*, we chose a targeted approach focused on *Bag3* for several reasons. First, genetic approaches to refine a QTL are complex and time consuming. Even with advanced genetic techniques they frequently fail to identify specific genes involved in regulation of the phenotype of interest. For example, other investigators have used such genetic approaches to narrow an associated QTL, *Canq1*,[10, 56] which was identified based on its association with collateral artery number in BL6 mice,[9]. The subsequent refined locus, *Dce1* (determinant of collateral extent 1), encompasses 737 kb and contains 28 genes.[56] Although *Bag3* is not contained within *Dce1*, this is likely due to the use of different surgical approaches to induce HLI and the fact that the phenotype of interest (collateral artery formation) may be distinct from the tissue

necrosis phenotype used in our studies and to define *Lsq-1*.[8] Second, evidence from our group and others supports a novel hypothesis for the etiology of tissue injury in limb ischemia in which the response of skeletal muscle cells to ischemia, and not solely tissue perfusion (e.g., collateral growth, arteriogenesis, or angiogenesis), is a critical determinant of whether skeletal muscle tissue survives an ischemic injury[16, 57]. Substantial evidence supports a role for BAG3 in the regulation of striated muscle function[20, 58–62], and mutations in BAG3 have been linked to both myofibrillar myopathy and dilated cardiomyopathy in humans, providing a strong rationale for targeted investigation of the effects of BAG3 variation on ischemia-induced muscle necrosis. Finally, although narrowing the *Lsq-1* locus (or related/overlapping loci) will be important, ultimately it will be necessary to tease out effects of individual target genes on specific phenotypes, whether limb muscle necrosis or collateral artery formation. It is unlikely that a single gene variant will explain the effects of *Lsq-1*, rather it is likely that *Lsq-1* is a complex association of genes that all contribute to the limb necrosis phenotype after HLI. For example, *Adam12*, another gene within *Lsq-1* that has also been linked to skeletal muscle regeneration,[63] was recently shown to be differentially expressed in BL6 and BALB/c mice and to regulate outcomes after HLI.[64] Although additional studies will be required to elucidate the complex genetic interactions among components of *Lsq-1*, such as *Bag3* and *Adam12*, our data demonstrate that variation in BAG3 is at least one critical component of this process.

The importance of BAG3 in the regulation of ischemic muscle cell survival was demonstrated by the significant beneficial effects of the BL6 variant, BAG3[Ile81], when exogenously expressed in BALB/c muscle. These results would appear to contrast with prior observations, in which *Bag3* heterozygous knockout mice displayed no differences in recovery from HLI compared to their wild-type littermates.[12] However, these mice were on a BL6 background, and as demonstrated previously, only a single BL6 allele is required for protection from ischemic injury,[8] thus it is not surprising that heterozygotes would behave like wild-type mice. Moreover, the finding in that report that postnatal day 7 *Bag3*$^{-/-}$ pups had no differences in pial collateral artery number or diameter reinforces our hypothesis that a primary effect of BAG3 is on skeletal muscle cells and not the vasculature. Global knockout alleles do not always provide clear insight into complex mechanisms of dysfunction that are caused by missense alleles, which is the focus of the current study. Consistent with our hypothesis, we showed that AAV6-mediated expression of BAG3 was largely localized to muscle cells and not endothelial cells, and mechanistically we demonstrated that BAG3[Ile81], but not BAG3[Met81], altered skeletal myoblast fusion and regeneration, which likely contributed to the beneficial effects on ischemic muscle survival. Furthermore, we demonstrated that BAG3[Ile81] had similar effects on muscle regeneration after cardiotoxin injection, a non-ischemic muscle injury model. Taken together, these findings demonstrate an important functional difference in the two BAG3 variants that appears to be at least partly responsible for the mouse strain-specific difference in ischemic injury. Moreover, they point to skeletal muscle regeneration as a potential novel target for the treatment of CLI patients. Whether variation in human *BAG3* confers susceptibility to muscle injury in PAD remains to be determined, but regardless of genetic differences in *BAG3* in humans, our results suggest that cellular processes regulated by BAG3, such as skeletal muscle cell integrity and regeneration, are important potential therapeutic targets.

The mechanistic basis for the functional differences between these two BAG3 variants is likely to involve differential protein-protein interactions that are altered by the presence of the hydrophobic methionine residue at position 81, which lies adjacent to one of two IPV domains in BAG3. These domains are involved in binding small heat shock proteins[29], which in turn are known to be involved in autophagy. We observed differences in expression of several autophagy-related proteins after ischemia in BALB/c and BL6 mice *in vivo* and in the context of the two BAG3 variants *in vitro*, suggesting a global effect of BAG[Ile81] on protein quality control. More importantly, however, differential binding of the small heat shock protein HspB8 to the BAG3 variants occurred *in vitro* in both myoblasts and differentiated myotubes, and functional analyses revealed a corresponding difference in ischemic muscle cell autophagic flux regulated by variants at residue 81. BAG3's role in autophagy is well-documented[28, 55, 61, 62], and autophagy is a critical process in muscle plasticity[34, 51–53]. In fact, autophagic flux is specifically linked to muscle satellite cell activity and the appearance of embryonic myosin heavy chain expression in regenerating dystrophic muscle [51]. The ability of the Ile81 variant to better facilitate autophagic flux may be directly responsible for the improved regenerative response induced by this variant in the setting of limb ischemia. Furthermore, improved autophagic flux may be a biological mechanism regulating the significantly improved myoblast fusion induced by BAG3[Ile81], as observed *in vivo* by eMyHC staining and *in vitro* in the myoblast fusion assay. BAG3 has also been shown to bind to components of the actin cytoskeleton[59], which could regulate membrane fusion events. Thus, it is possible that differential protein binding by the two variants could be responsible for additional functional differences between these two BAG3 variants. Importantly, the Met81 variant did not act as a dominant inhibitor of any of BAG3's putative functions in BL6 mice. These findings support a beneficial protective function mediated specifically by the Ile81 variant.

It is intriguing to note that capillary density was also increased in mice treated with AAV-BAG[Ile81]. Although we saw efficient expression of our AAV in myofibers, we observed no immunofluorescence co-labeling of CD31^{+}, SMA^{+}, and our FLAG-tagged construct, suggesting that our AAV6 serotype more efficiently infected and/or expressed in muscle cells *in vivo*. It is possible that improved muscle cell survival resulted in enhanced ischemia-induced expression of vascular growth factors and subsequent angiogenesis[65, 66]. Prior studies of murine HLI have supported the idea that pre-existing collateral vessels and arteriogenesis are critical determinants of necrosis and perfusion recovery [67, 68]. However, other physiological mechanisms also play a role in these processes. Specifically, the modulation of infarct volume by the *Lsq-1* candidate gene *IL21R* after cerebral ischemia occurs in part through a non-vascular neuroprotective mechanism[69], which parallels our observations regarding BAG3 and skeletal muscle during limb ischemia. The expression of BAG3[Ile81] could alter expression of other factors within the *Lsq-1* QTL, such as *Adam12* or *IL21R*. In addition to ADAM12's role in muscle progenitor cell biology and muscle regeneration, members of our group have recently shown that ADAM12 modulates endothelial cell function and angiogenesis during ischemia[14]. Whether BAG3 modulates ADAM12 expression or function directly or indirectly as a result of preserved muscle function and/or improved regeneration is not known, but exploration of such interactions

among genes within *Lsq-1* will be important to fully understand its role in regulating limb muscle survival in ischemia.

In conclusion, our data demonstrate that *Bag3* is an important regulator of murine limb tissue necrosis following HLI. HLI is characterized by rapid onset of tissue ischemia, which contrasts with clinical PAD where ischemia develops gradually over the course of years as a result of chronic atherosclerosis. Despite this difference, clinical CLI is characterized by marked tissue injury similar to that observed in the acute HLI model, thus our data strongly support *Bag3* as a candidate for the regulation of tissue injury and recovery during PAD. Overall, these findings are an important initial step in understanding the complex multi-tissue pathology of CLI and provide critical insights into genetic determinants that may lead to diagnostic and therapeutic interventions for this devastating disease.

Supplementary Material

Refer to Web version on PubMed Central for supplementary material.

Acknowledgments

References

1. Gabel S, Benefield J, Meisinger J, Petruzzelli GJ, Young M. Protein phosphatases 1 and 2A maintain endothelial cells in a resting state, limiting the motility that is needed for the morphogenic process of angiogenesis. Otolaryngol Head Neck Surg. 1999; 121:463–468. [PubMed: 10504605]

2. Gudmundsson G, Matthiasson SE, Arason H, Johannsson H, Runarsson F, Bjarnason H, Helgadottir K, Thorisdottir S, Ingadottir G, Lindpaintner K, Sainz J, Gudnason V, Frigge ML, Kong A, Gulcher JR, Stefansson K. Localization of a gene for peripheral arterial occlusive disease to chromosome 1p31. Am J Hum Genet. 2002; 70:586–592. [PubMed: 11833003]

3. Katwal AB, Dokun AO. Peripheral arterial disease in diabetes: is there a role for genetics? Curr Diab Rep. 2011; 11:218–225. [PubMed: 21424681]

4. Knowles JW, Assimes TL, Li J, Quertermous T, Cooke JP. Genetic susceptibility to peripheral arterial disease: a dark corner in vascular biology. Arterioscler Thromb Vasc Biol. 2007; 27:2068–2078. [PubMed: 17656669]

5. Leeper NJ, Kullo IJ, Cooke JP. Genetics of peripheral artery disease. Circulation. 2012; 125:3220–3228. [PubMed: 22733336]

6. Messina LM. Elucidating the genetic basis of peripheral arterial disease: identification of a quantitative trait locus that determines the phenotypic response to experimental hindlimb ischemia. Circulation. 2008; 117:1127–1129. [PubMed: 18316497]

7. Matzke S, Lepantalo M. Claudication does not always precede critical leg ischemia. Vasc Med. 2001; 6:77–80. [PubMed: 11530968]

8. Dokun AO, Keum S, Hazarika S, Li Y, Lamonte GM, Wheeler F, Marchuk DA, Annex BH. A quantitative trait locus (LSq-1) on mouse chromosome 7 is linked to the absence of tissue loss after surgical hindlimb ischemia. Circulation. 2008; 117:1207–1215. [PubMed: 18285563]

9. Wang S, Zhang H, Dai X, Sealock R, Faber JE. Genetic architecture underlying variation in extent and remodeling of the collateral circulation. Circ Res. 2010; 107:558–568. [PubMed: 20576932]

10. Wang S, Zhang H, Wiltshire T, Sealock R, Faber JE. Genetic dissection of the Canq1 locus governing variation in extent of the collateral circulation. PLoS ONE. 2012; 7:e31910. [PubMed: 22412848]

11. Chalothorn D, Clayton JA, Zhang H, Pomp D, Faber JE. Collateral density, remodeling, and VEGF-A expression differ widely between mouse strains. Physiol Genomics. 2007; 30:179–191. [PubMed: 17426116]

12. Chalothorn D, Faber JE. Strain-dependent variation in collateral circulatory function in mouse hindlimb. Physiol Genomics. 2010; 42:469–479. [PubMed: 20551146]

13. Keum S, Marchuk DA. A locus mapping to mouse chromosome 7 determines infarct volume in a mouse model of ischemic stroke. Circ Cardiovasc Genet. 2009; 2:591–598. [PubMed: 20031639]

14. Dokun AO, Chen L, Okutsu M, Farber CR, Hazarika S, Jones WS, Craig D, Marchuk DA, Lye RJ, Shah SH, Annex BH. ADAM12: A Genetic Modifier of Pre-clinical Peripheral Arterial Disease. Am J Physiol Heart Circ Physiol. 2015 Sep; 309(5):H790–803. [PubMed: 26163448]

15. Wang T, Cunningham A, Dokun AO, Hazarika S, Houston K, Chen L, Lye RJ, Spolski R, Leonard WJ, Annex BH. Loss of interleukin-21 receptor activation in hypoxic endothelial cells impairs perfusion recovery after hindlimb ischemia. Arterioscler Thromb Vasc Biol. 2015; 35:1218–1225. [PubMed: 25838422]

16. McClung JM, McCord TJ, Keum S, Johnson S, Annex BH, Marchuk DA, Kontos CD. Skeletal muscle-specific genetic determinants contribute to the differential strain-dependent effects of hindlimb ischemia in mice. Am J Pathol. 2012; 180:2156–2169. [PubMed: 22445571]

17. McDermott MM, Ferrucci L, Guralnik J, Tian L, Liu K, Hoff F, Liao Y, Criqui MH. Pathophysiological changes in calf muscle predict mobility loss at 2-year follow-up in men and women with peripheral arterial disease. Circulation. 2009; 120:1048–1055. [PubMed: 19738138]

18. McDermott MM, Guralnik JM, Ferrucci L, Tian L, Pearce WH, Hoff F, Liu K, Liao Y, Criqui MH. Physical activity, walking exercise, and calf skeletal muscle characteristics in patients with peripheral arterial disease. J Vasc Surg. 2007; 46:87–93. [PubMed: 17540532]

19. McDermott MM, Liu K, Tian L, Guralnik JM, Criqui MH, Liao Y, Ferrucci L. Calf muscle characteristics, strength measures, and mortality in peripheral arterial disease: a longitudinal study. J Am Coll Cardiol. 2012; 59:1159–1167. [PubMed: 22440216]

20. Homma S, Iwasaki M, Shelton GD, Engvall E, Reed JC, Takayama S. BAG3 deficiency results in fulminant myopathy and early lethality. Am J Pathol. 2006; 169:761–773. [PubMed: 16936253]

21. Lee H, Cherk S, Chan S, Wong S, Tong T, Ho W, Chan A, Lee K, Mak C. BAG3-related myofibrillar myopathy in a Chinese family. Clin Genet. 2012; 81(4):394–398. [PubMed: 21361913]

22. Selcen D, Muntoni F, Burton BK, Pegoraro E, Sewry C, Bite AV, Engel AG. Mutation in BAG3 causes severe dominant childhood muscular dystrophy. Ann Neurol. 2009; 65:83–89. [PubMed: 19085932]

23. Hishiya A, Kitazawa T, Takayama S. BAG3 and Hsc70 interact with actin capping protein CapZ to maintain myofibrillar integrity under mechanical stress. Circ Res. 2010; 107:1220–1231. [PubMed: 20884878]

24. Norton N, Li D, Rieder MJ, Siegfried JD, Rampersaud E, Zuchner S, Mangos S, Gonzalez-Quintana J, Wang L, McGee S, Reiser J, Martin E, Nickerson DA, Hershberger RE. Genome-wide studies of copy number variation and exome sequencing identify rare variants in BAG3 as a cause of dilated cardiomyopathy. Am J Hum Genet. 2011; 88:273–282. [PubMed: 21353195]

25. Villard E, Perret C, Gary F, Proust C, Dilanian G, Hengstenberg C, Ruppert V, Arbustini E, Wichter T, Germain M, Dubourg O, Tavazzi L, Aumont MC, DeGroote P, Fauchier L, Trochu JN, Gibelin P, Aupetit JF, Stark K, Erdmann J, Hetzer R, Roberts AM, Barton PJ, Regitz-Zagrosek V, Aslam U, Duboscq-Bidot L, Meyborg M, Maisch B, Madeira H, Waldenstrom A, Galve E, Cleland JG, Dorent R, Roizes G, Zeller T, Blankenberg S, Goodall AH, Cook S, Tregouet DA, Tiret L, Isnard R, Komajda M, Charron P, Cambien F. A genome-wide association study identifies two loci associated with heart failure due to dilated cardiomyopathy. Eur Heart J. 2011; 32:1065–1076. [PubMed: 21459883]

26. Homma S, Iwasaki M, Shelton GD, Engvall E, Reed JC, Takayama S. BAG3 deficiency results in fulminant myopathy and early lethality. Am J Pathol. 2006; 169:761–773. [PubMed: 16936253]

27. Carra S, Seguin SJ, Lambert H, Landry J. HspB8 chaperone activity toward poly(Q)-containing proteins depends on its association with Bag3, a stimulator of macroautophagy. J Biol Chem. 2008; 283:1437–1444. [PubMed: 18006506]

28. Carra S, Seguin SJ, Landry J. HspB8 and Bag3: a new chaperone complex targeting misfolded proteins to macroautophagy. Autophagy. 2008; 4:237–239. [PubMed: 18094623]

29. Fuchs M, Poirier DJ, Seguin SJ, Lambert H, Carra S, Charette SJ, Landry J. Identification of the key structural motifs involved in HspB8/HspB6-Bag3 interaction. Biochem J. 2010; 425:245–255.

30. Gamerdinger M, Carra S, Behl C. Emerging roles of molecular chaperones and co-chaperones in selective autophagy: focus on BAG proteins. J Mol Med (Berl). 2011; 89:1175–1182. [PubMed: 21818581]

31. Gamerdinger M, Hajieva P, Kaya AM, Wolfrum U, Hartl FU, Behl C. Protein quality control during aging involves recruitment of the macroautophagy pathway by BAG3. EMBO J. 2009; 28:889–901. [PubMed: 19229298]

32. Standards of medical care in diabetes. Diabetes Care. 2004; 27(Suppl 1):S15–35. [PubMed: 14693923]

33. Moresi V, Carrer M, Grueter CE, Rifki OF, Shelton JM, Richardson JA, Bassel-Duby R, Olson EN. Histone deacetylases 1 and 2 regulate autophagy flux and skeletal muscle homeostasis in mice. Proc Natl Acad Sci U S A. 2012; 109:1649–1654. [PubMed: 22307625]

34. Masiero E, Agatea L, Mammucari C, Blaauw B, Loro E, Komatsu M, Metzger D, Reggiani C, Schiaffino S, Sandri M. Autophagy is required to maintain muscle mass. Cell Metab. 2009; 10:507–515. [PubMed: 19945408]

35. Zhang X, Yan H, Yuan Y, Gao J, Shen Z, Cheng Y, Shen Y, Wang RR, Wang X, Hu WW, Wang G, Chen Z. Cerebral ischemia-reperfusion-induced autophagy protects against neuronal injury by mitochondrial clearance. Autophagy. 2013; 9:1321–1333. [PubMed: 23800795]

36. Przyklenk K, Dong Y, Undyala VV, Whittaker P. Autophagy as a therapeutic target for ischaemia/reperfusion injury? Concepts, controversies, and challenges. Cardiovasc Res. 2012; 94:197–205. [PubMed: 22215722]

37. Keum S, Lee HK, Chu PL, Kan MJ, Huang MN, Gallione CJ, Gunn MD, Lo DC, Marchuk DA. Natural genetic variation of integrin alpha L (Itgal) modulates ischemic brain injury in stroke. PLoS Genet. 2013; 9:e1003807. [PubMed: 24130503]

38. Yan Z, Choi S, Liu X, Zhang M, Schageman JJ, Lee SY, Hart R, Lin L, Thurmond FA, Williams RS. Highly coordinated gene regulation in mouse skeletal muscle regeneration. J Biol Chem. 2003; 278:8826–36. [PubMed: 12477723]

39. Fontijn R, Hop C, Brinkman HJ, Slater R, Westerveld A, van Mourik JA, Pannekoek H. Maintenance of vascular endothelial cell-specific properties after immortalization with an amphotrophic replication-deficient retrovirus containing human papilloma virus 16 E6/E7 DNA. Exp Cell Res. 1995; 216:199–207. [PubMed: 7813621]

40. McClung JM, McCord TJ, Keum S, Johnson S, Annex BH, Marchuk DA, Kontos CD. Skeletal muscle-specific genetic determinants contribute to the differential strain-dependent effects of hindlimb ischemia in mice. Am J Pathol. 2012; 180:2156–2169. [PubMed: 22445571]

41. Spangenburg EE, Le Roith D, Ward CW, Bodine SC. A functional insulin-like growth factor receptor is not necessary for load-induced skeletal muscle hypertrophy. J Physiol. 2008; 586:283–291. [PubMed: 17974583]

42. Kimura S, Noda T, Yoshimori T. Dissection of the autophagosome maturation process by a novel reporter protein, tandem fluorescent-tagged LC3. Autophagy. 2007; 3:452–460. [PubMed: 17534139]

43. Zhang P, Verity MA, Reue K. Lipin-1 regulates autophagy clearance and intersects with statin drug effects in skeletal muscle. Cell Metab. 2014; 20:267–279. [PubMed: 24930972]

44. Ryan TE, Schmidt CA, Alleman RJ, Tsang AM, Green TD, Neufer PD, Brown DA, McClung JM. Mitochondrial therapy improves limb perfusion and myopathy following hindlimb ischemia. J Mol Cell Cardiol. 2016; 97:191–196. [PubMed: 27262673]

45. Ryan TE, Schmidt CA, Green TD, Spangenburg EE, Neufer PD, McClung JM. Targeted expression of Catalase to Mitochondria Protects Against Ischemic Myopathy in High Fat Fed Mice. Diabetes. 2016; 65(9):2553–2568. [PubMed: 27284110]

46. Schmidt AS, Ryan TE, Lin CT, Inigo MMR, Green TD, Brault JJ, Spangenburg EE, McClung JM. Diminished force production and mitochondrial respiratory deficits are strain-dependent myopathies of subacute limb ischemia. J Vasc Surg. 2016; pii: S0741-5214(16)30193-8. doi: 10.1016/j.jvs.2016.04.041

47. Clayton JA, Chalothorn D, Faber JE. Vascular endothelial growth factor-A specifies formation of native collaterals and regulates collateral growth in ischemia. Circ Res. 2008; 103:1027–1036. [PubMed: 18802023]

48. Zhang H, Prabhakar P, Sealock R, Faber JE. Wide genetic variation in the native pial collateral circulation is a major determinant of variation in severity of stroke. J Cereb Blood Flow Metab. 2010; 30:923–934. [PubMed: 20125182]

49. Lee HC, Cherk SW, Chan SK, Wong S, Tong TW, Ho WS, Chan AY, Lee KC, Mak CM. BAG3-related myofibrillar myopathy in a Chinese family. Clin Genet. 2012; 81:394–398. [PubMed: 21361913]

50. Odgerel Z, Sarkozy A, Lee HS, McKenna C, Rankin J, Straub V, Lochmuller H, Paola F, D'Amico A, Bertini E, Bushby K, Goldfarb LG. Inheritance patterns and phenotypic features of myofibrillar myopathy associated with a BAG3 mutation. Neuromuscular disorders. 2010; 20:438–442. [PubMed: 20605452]

51. Fiacco E, Castagnetti F, Bianconi V, Madaro L, De Bardi M, Nazio F, D'Amico A, Bertini E, Cecconi F, Puri PL, Latella L. Autophagy regulates satellite cell ability to regenerate normal and dystrophic muscles. Cell Death Differ. 2016; 23:1839–1849. [PubMed: 27447110]

52. Sandri M. Autophagy in skeletal muscle. FEBS Lett. 2010; 584:1411–1416. [PubMed: 20132819]

53. Sandri M, Coletto L, Grumati P, Bonaldo P. Misregulation of autophagy and protein degradation systems in myopathies and muscular dystrophies. J Cell Sci. 2013; 126:5325–5333. [PubMed: 24293330]

54. Sachdev U, Cui X, Hong G, Namkoong S, Karlsson JM, Baty CJ, Tzeng E. High mobility group box 1 promotes endothelial cell angiogenic behavior in vitro and improves muscle perfusion in vivo in response to ischemic injury. J Vasc Surg. 2012; 55:180–191. [PubMed: 21944908]

55. Behl C. BAG3 and friends: co-chaperones in selective autophagy during aging and disease. Autophagy. 2011; 7:795–798. [PubMed: 21681022]

56. Sealock R, Zhang H, Lucitti JL, Moore SM, Faber JE. Congenic fine-mapping identifies a major causal locus for variation in the native collateral circulation and ischemic injury in brain and lower extremity. Circ Res. 2014; 114:660–671. [PubMed: 24300334]

57. McClung JM, McCord TJ, Southerland K, Schmidt CA, Padgett ME, Ryan TE, Kontos CD. Subacute limb ischemia induces skeletal muscle injury in genetically susceptible mice independent of vascular density. J Vasc Surg. 2016; 64(4):1101–1111. [PubMed: 26254821]

58. Feldman AM, Gordon J, Wang J, Song J, Zhang XQ, Myers VD, Tilley DG, Gao E, Hoffman NE, Tomar D, Madesh M, Rabinowitz J, Koch WJ, Su F, Khalili K, Cheung JY. BAG3 regulates contractility and Ca(2+) homeostasis in adult mouse ventricular myocytes. J Mol Cell Cardiol. 2016; 92:10–20. [PubMed: 26796036]

59. Hishiya A, Kitazawa T, Takayama S. BAG3 and Hsc70 interact with actin capping protein CapZ to maintain myofibrillar integrity under mechanical stress. Circ Res. 2010; 107:1220–1231. [PubMed: 20884878]

60. Quintana MT, Parry TL, He J, Yates CC, Sidorova TN, Murray KT, Bain JR, Newgard CB, Muehlbauer MJ, Eaton SC, Hishiya A, Takayama S, Willis MS. Cardiomyocyte-Specific Human Bcl2-Associated Anthanogene 3 P209L Expression Induces Mitochondrial Fragmentation, Bcl2-Associated Anthanogene 3 Haploinsufficiency, and Activates p38 Signaling. Am J Pathol. 2016; 186(8):1989–2007. [PubMed: 27321750]

61. Tahrir FG, Knezevic T, Gupta MK, Gordon J, Cheung JY, Feldman AM, Khalili K. Evidence for the Role of BAG3 in Mitochondrial Quality Control in Cardiomyocytes. J Cell Physiol. 2017 Apr; 232(4):797–805. [PubMed: 27381181]

62. Zhang J, He Z, Xiao W, Na Q, Wu T, Su K, Cui X. Overexpression of BAG3 Attenuates Hypoxia-Induced Cardiomyocyte Apoptosis by Inducing Autophagy. Cell Physiol Biochem. 2016; 39:491–500. [PubMed: 27383426]

63. Lafuste P, Sonnet C, Chazaud B, Dreyfus PA, Gherardi RK, Wewer UM, Authier FJ. ADAM12 and alpha9beta1 integrin are instrumental in human myogenic cell differentiation. Mol Biol Cell. 2005; 16:861–870. [PubMed: 15574885]

64. Dokun AO, Chen L, Okutsu M, Farber CR, Hazarika S, Jones WS, Craig D, Marchuk DA, Lye RJ, Shah SH, Annex BH. ADAM12: a genetic modifier of preclinical peripheral arterial disease. Am J Physiol Heart Circ Physiol. 2015; 309:H790–803. [PubMed: 26163448]

65. Mofarrahi M, McClung JM, Kontos CD, Davis EC, Tappuni B, Moroz N, Pickett AE, Huck L, Harel S, Danialou G, Hussain SN. Angiopoietin-1 Enhances Skeletal Muscle Regeneration in Mice. Am J Physiol Regul Integr Comp Physiol. 2015; 308(7):R576–589. pr 1. [PubMed: 25608750]

66. McClung JM, Reinardy JL, Mueller SB, McCord TJ, Kontos CD, Brown DA, Hussain SN, Schmidt CA, Ryan TE, Green TD. Muscle cell derived angiopoietin-1 contributes to both myogenesis and angiogenesis in the ischemic environment. Front Physiol. 2015; 6:161. [PubMed: 26042050]

67. Mac Gabhann F, Peirce SM. Collateral capillary arterialization following arteriolar ligation in murine skeletal muscle. Microcirculation. 2010; 17:333–347. [PubMed: 20618691]

68. Scholz D, Ziegelhoeffer T, Helisch A, Wagner S, Friedrich C, Podzuweit T, Schaper W. Contribution of arteriogenesis and angiogenesis to postocclusive hindlimb perfusion in mice. J Mol Cell Cardiol. 2002; 34:775–787. [PubMed: 12099717]

69. Lee HK, Keum S, Sheng H, Warner DS, Lo DC, Marchuk DA. Natural allelic variation of the IL-21 receptor modulates ischemic stroke infarct volume. J Clin Invest. 2016; 126(8):2827–2838. [PubMed: 27400126]

Clinical Perspective

What is new?

- Recent evidence suggests that genetic differences may play a key role in the susceptibility to peripheral arterial disease.

- Bcl-2-associated athanogene-3 (BAG3) is a cell chaperone protein previously identified in a genetic screen for determinants of tissue loss with hindlimb ischemia.

- Using adeno-associated viruses (AAV), we show that an isoleucine to methionine variant at position 81 in BAG3 is sufficient to confer susceptibility to ischemic tissue necrosis in BALB/c mice.

- This work demonstrates that BAG3, a gene with known polymorphisms that cause human myofibrillar and cardiac myopathies, is a modulator of ischemic muscle necrosis and blood flow.

What are the clinical implications?

- The susceptibility of BALB/c and other inbred mouse strains to ischemia has been used as a model of human critical limb ischemia.

- Therapies of this nature could be utilized independently or in concert with current interventions (endovascular, revascularization) to reduce morbidity/ mortality in all clinical manifestations of PAD.
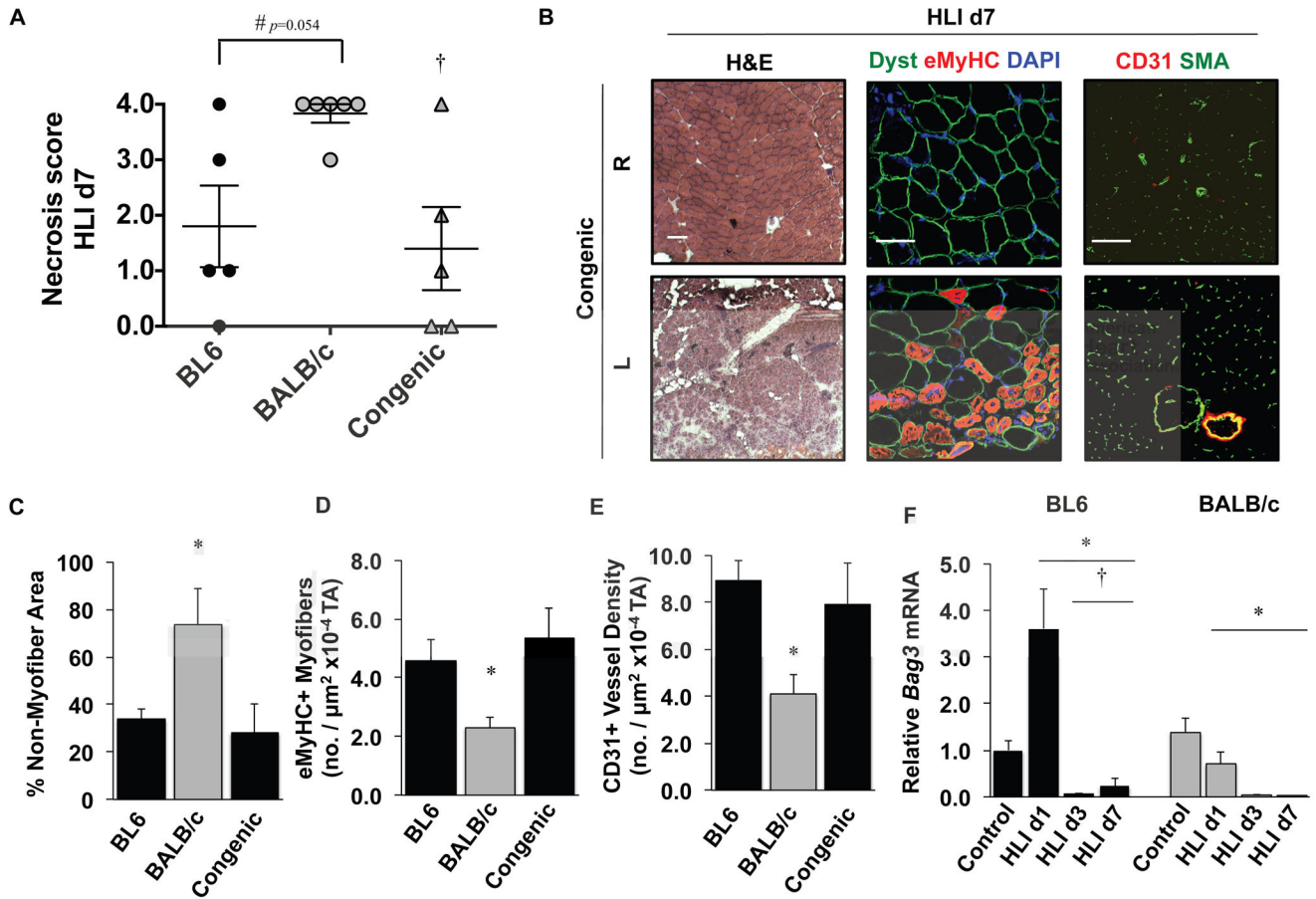
Figure 1. Identification of *Bag3* as a target for HLI-induced tissue necrosis

A. BL6, BALB/c, and Congenic mice (C.B6-*Lsq1-3,* also known as *C.B6-Civq1-3;* N 5 mice per strain) were subjected to HLI and limb necrosis was assessed using a semi-quantitative scoring system. #*P*=NS (0.054) vs. BL6. †*P*<0.05 vs. BALB/c. **B**. Representative images of Congenic contralateral control (R) and ischemic limb (L) muscle morphology (H&E), regeneration (dystrophin, eMyHC), and vascular morphology (CD31, SMA). Dyst, dystrophin (N=4 mice/strain, scale bar = 100μm). **C–E.** Quantification of strain dependent non-myofiber area (**C**), eMyHC^{+} myofibers (**D**), and CD31^{+} density (**E**) on d7 after HLI (N=4 mice/strain). *P<0.05 vs. BL6 and Congenic. **F.** Gastrocnemius BAG3 mRNA expression (corrected for GAPDH and normalized to BL6 control) after HLI in BL6 (black bars) and BALB/c (gray bars) mice (N=4 mice/strain/day). *P<0.05 vs. strain-specific Control. †P<0.05 vs. strain-specific HLI d1. Necrosis data plotted per mouse, with means ± SEM. All other data are means ± SEM.
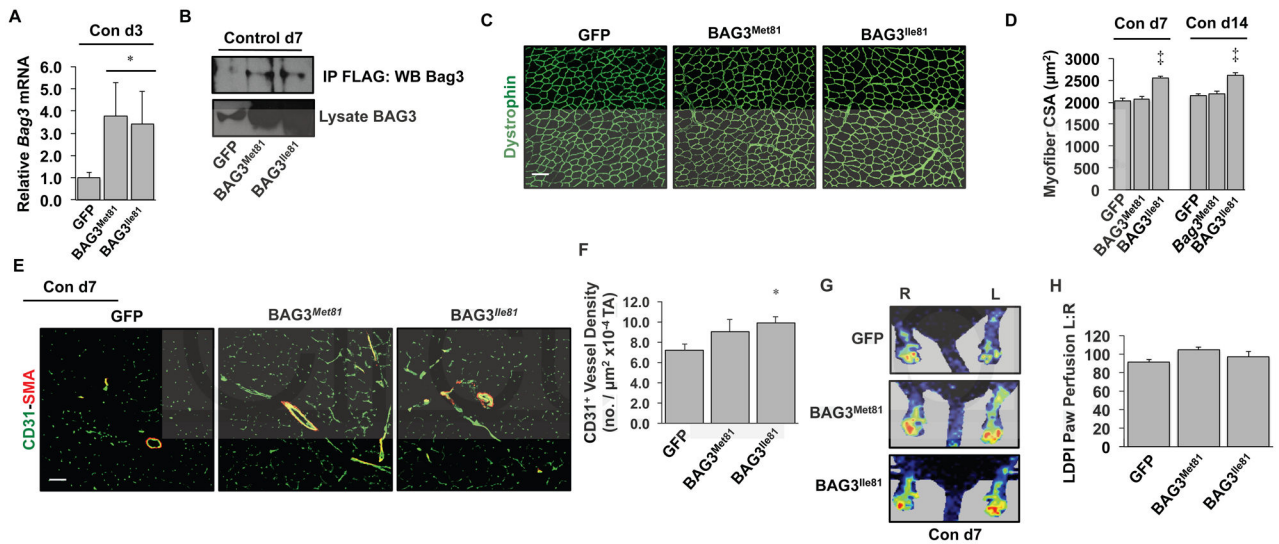
Figure 2. Strain-specific coding variants of BAG3 differentially promote limb muscle hypertrophy and capillary density in non-ischemic muscle

A–B. Intramuscular injection into BALB/c mice of adeno-associated viruses encoding BAG3^{Met81} or BAG3^{Ile81} (N=4 mice/virus) resulted in similar upregulation of *Bag3* mRNA on day 3 post-injection (**A**) and FLAG-tagged BAG3 protein on day 7 post-injection (**B**) compared to mice injected with AAV-GFP. * *P*<0.05 vs. GFP. IP, immunoprecipitation; WB, western blot. **C.** Representative dystrophin staining (pseudocolored green; scale bar=100 μm) of TA muscle 14 days post-injection. **D.** Quantification of myofiber CSA on days 7 and 14 post-injection (N=4 mice/virus). ‡ *P*<0.05 vs. GFP or BAG3^{Met81}. **E.** Representative images of CD31 and smooth muscle actin (SMA) staining 7 days post-injection (scale bar=100 μm). **F.** Quantification of CD31$^+$ vessel density in TA muscle. *, *P*<0.05 vs. GFP (N=4 mice/virus). **G–H.** Limb perfusion was analyzed by LDPI on day 7 post-injection (N=10 mice/virus) (**G**) and quantified (**H**) as a percentage of perfusion in the non-injected limb.
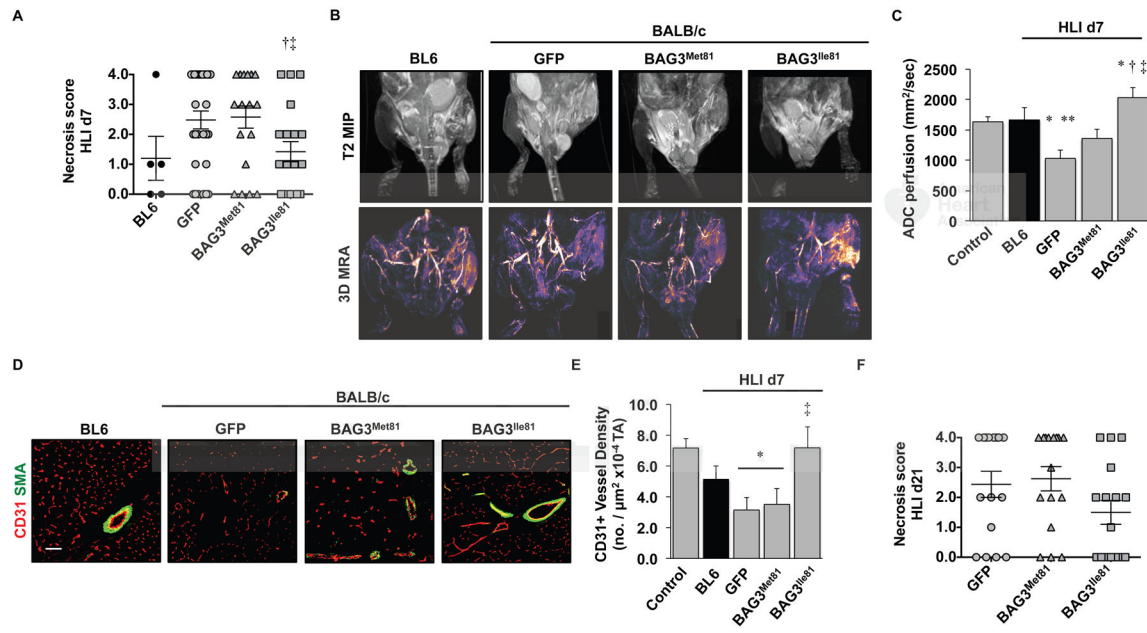
Figure 3. BAG3^{Ile81} expression regulates ischemic limb tissue necrosis and perfusion
BL6 (N=5) and BALB/c mice were injected IM with AAVs (N=29 GFP; N=19 BAG3^{Met81}; N=19 BAG3^{Ile81}) and 7 days later subjected to HLI. **A**. Semi-quantitative scoring of limb muscle necrosis. †P<0.05 vs. GFP; ‡ P<0.05 vs. BAG3^{Met81}. **B**. Representative MR T2-weighted and MR angiography images and (**C**) quantification of MR ADC perfusion at HLI d7 (N=4 BL6; N=8 GFP; N=7 BAG3^{Met81}; N=6 BAG3^{Ile81}). *P<0.05 vs. Control; **P<0.05 vs. BL6; †P<0.05 vs. GFP; ‡ P<0.05 vs. BAG3^{Met81}. **D**. Representative images of CD31 and SMA staining (scale bar=100μm) (**D**) for quantification of CD31$^+$ vessel density (**E**) at HLI d7 (N 4 mice/group). *P<0.05 vs. Control; ‡ P<0.05 vs. GFP or BAG3^{Met81}. **F**. Virus-injected BALB/c mice (N=16 mice/virus) were subjected to HLI for 21d, and limb necrosis score data plotted per mouse, with means ± SEM. All other data are means ± SEM.
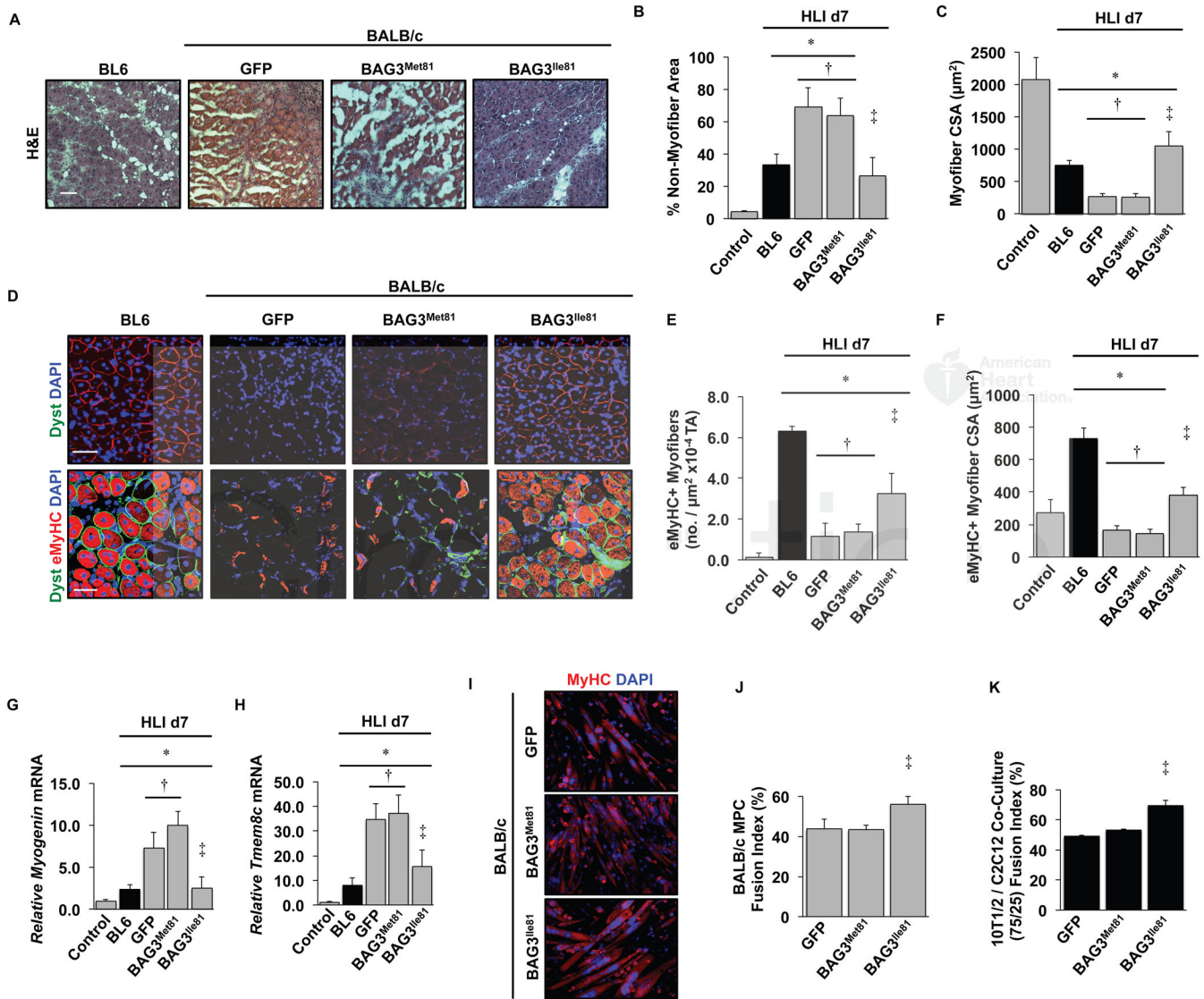
Figure 4. BAG3^Ile81 rescues ischemic BALB/c muscle morphology and regeneration

BL6 (black bars) and BALB/c (gray bars) mice injected IM with AAVs were subjected to HLI for 7 days. The TA was analyzed histologically (H&E, **A**, scale bar=100μm), and non-myofiber area (**B**) and myofiber cross sectional area (**C**) were quantified (N ≥ 5 mice/group). Note the lack of fascicular myofiber arrangement and absence of centralized myofiber nuclei in GFP and BAG3^Met81 groups, which were rescued by BAG3^Met81. **D**. Representative immunofluorescence images of TA muscle labeled with antibodies against embryonic heavy chain (eMyHC) and dystrophin (pseudocolored green scale bar=100μm) were used to quantify eMyHC⁺ myofiber number (**E**) and size (**F**) (N ≥ 5 mice/group). There were very few eMyHC⁺ fibers in contralateral non-ischemic control limbs. **G–H**. Gastrocnemius mRNA expression of myogenin (**G**) and Tmem8c (myomaker) (**H**) were determined by qRT-PCR (N ≥ 5 mice/group, corrected for GAPDH and normalized to contralateral control). **I**. Representative images of primary muscle progenitor cells from BALB/c mice that were infected with AAVs encoding GFP, BAG3^Met81, or BAG3^Ile81 then differentiated into

myotubes and labeled with DAPI and anti-MyHC (N 3 group). **J**. Quantification of myoblast fusion index. **K.** Quantification of fusion index for C3H-10T1/2 pluripotent pericyte cells and C2C12 myoblasts mixed at a 75:25 ratio and infected with the indicated AAVs (N 3 group). *P<0.05 vs. Control; †P<0.05 vs. BL6; ‡ P<0.05 vs. GFP or BAG3[Met81]. All data are means ± SEM.
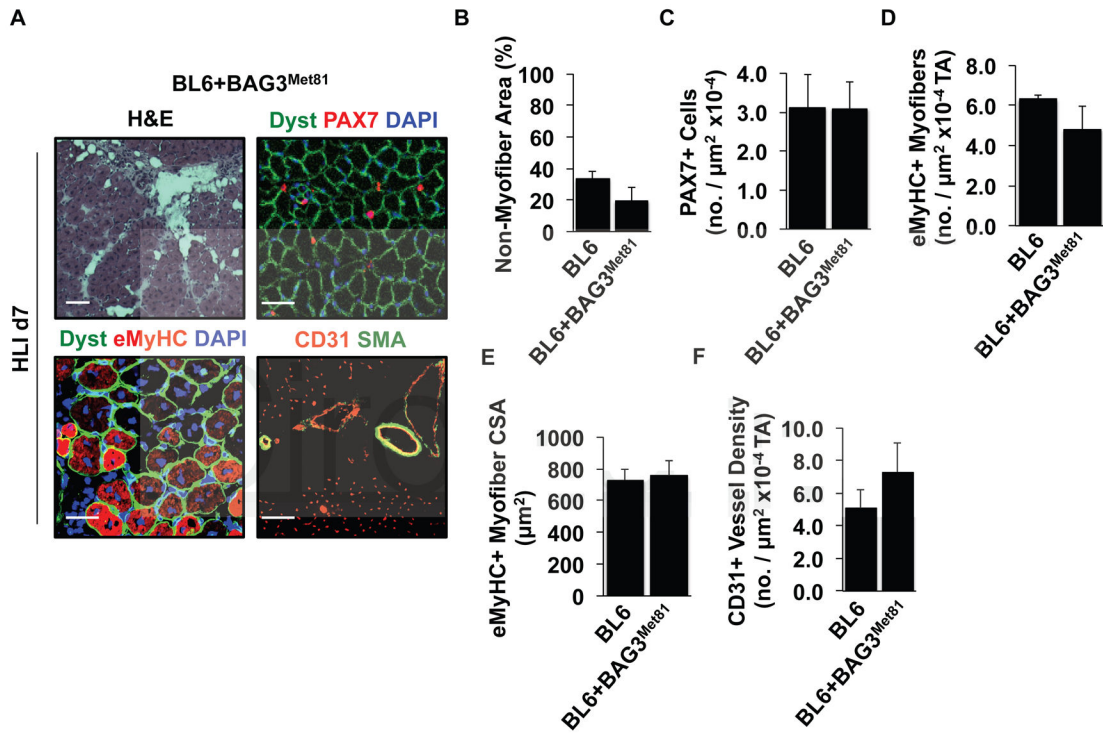
Figure 5. BAG3^Met81 is not a dominant negative inhibitor in ischemic BL6 muscle
BL6 mice were infected with AAV6 encoding BAG^{Met81} for 7 days and subjected to 7 days of HLI (N 5 mice/group). **A**. Representative H&E-stained and IF images labeled for dystrophin, PAX7, eMyHC, CD31, and SMA (scale bar=100μm) were used to quantify non-myofiber tissue area (**B**), PAX7$^+$ nuclei (**C**), eMyHC expression (**D**), size of eMyHC$^+$ myofibers (**E**), and capillary density (**F**). All data are means ± SEM.
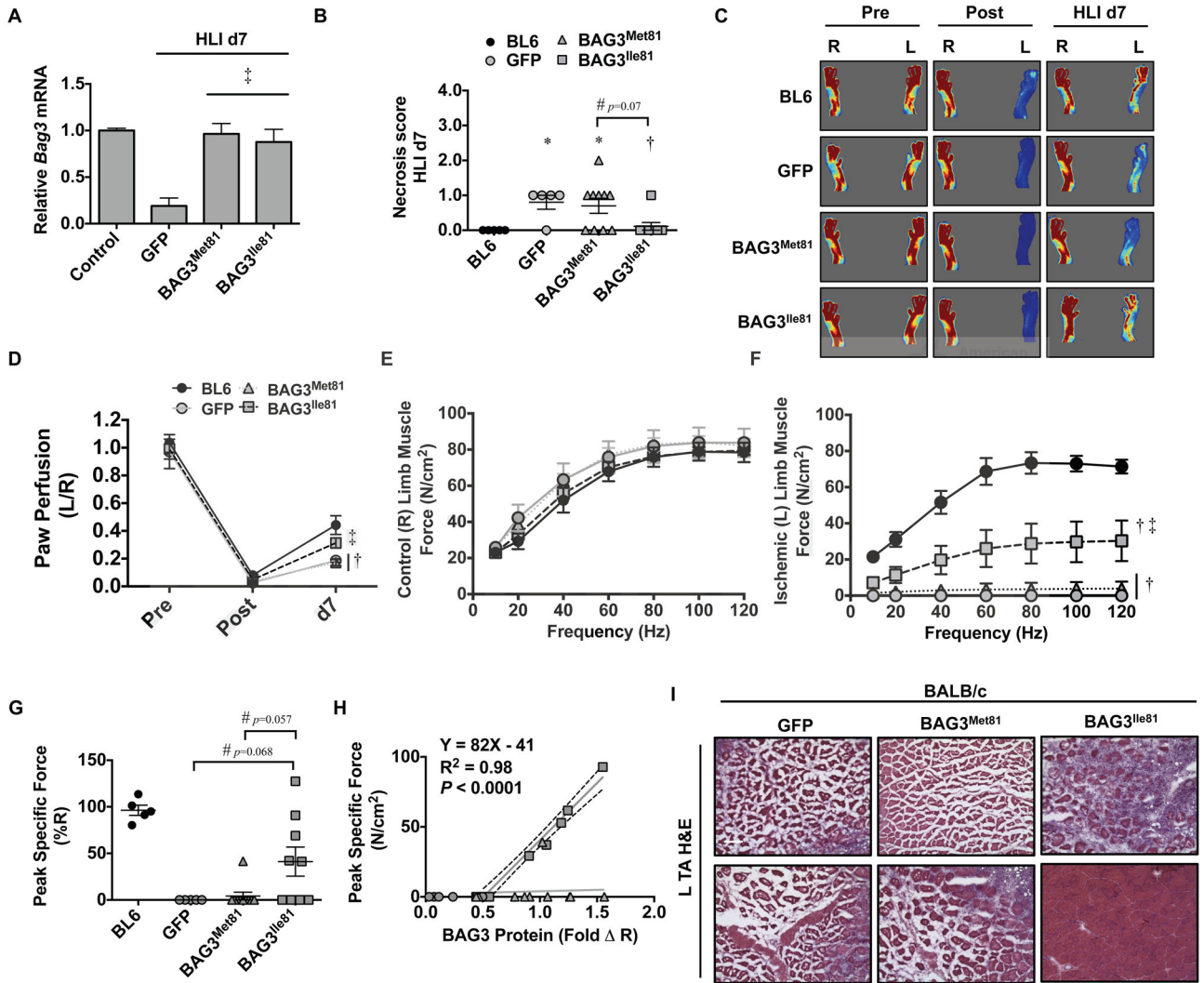
Figure 6. Systemic BAG3^Ile81 delivery rescues BALB/c limb muscle blood flow and function after ischemia

BL6 (black bars, N=5) and BALB/c (gray bars) mice injected IV with AAVs encoding GFP (N=5), BAG3^Met81 (N=10), or BAG3^Ile81 (N=9) were subjected to modified HLI with collateral vessels left intact. **A**. Quantification of skeletal muscle BAG3 mRNA expression by qRT-PCR, corrected for GAPDH and normalized to contralateral control. **B**. Limb necrosis score data plotted per mouse, with means ± SEM. *$P<0.05$ vs. BL6. #P=NS (0.07). †$P<0.05$ vs. GFP. **C.** Representative LDPI images of paw blood flow. **D**. Quantification of paw perfusion by LDPI. **E–F**. Force-frequency analysis of isolated extensor digitorum longus (EDL) muscles from the contralateral control (**E**) and ischemic (**F**) limbs at HLI d7. **G**. Peak specific EDL muscle force (expressed as a % of the contralateral EDL). BL6 peak specific force values presented only as a frame of reference. #P=NS (0.068), Ile v GFP. #P=NS (0.057), Ile v Met. **H**. Correlational analysis between BAG3 protein expression and muscle peak specific force. Line fit by least square regression. **I**. Representative H&E stains for TA muscle morphological analysis (scale bar=100μm). $P<0.05$ vs. BL6; ‡ $P<0.05$ vs. GFP or BAG3^Met81. All other data are means ± SEM.
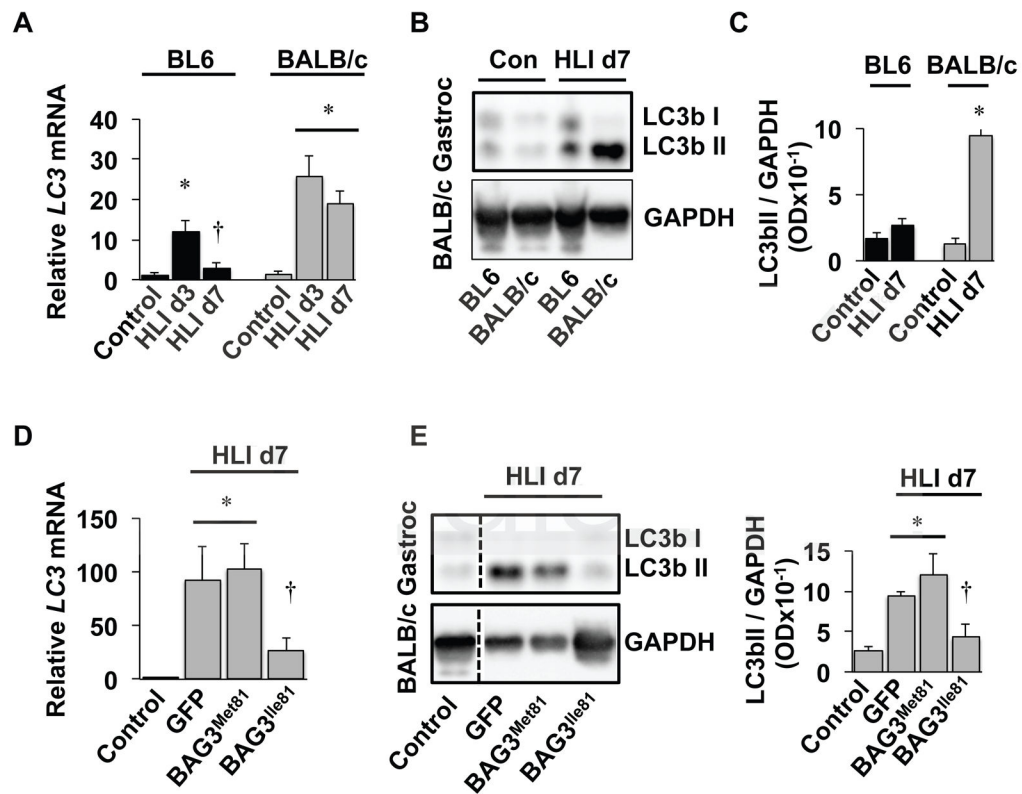
Figure 7. Autophagy is differentially regulated in ischemic BALB/c and BL6 muscle and by BAG3 variants

A. BL6 and BALB/c mice were subjected to HLI for 3 or 7-days (N 5 mice per strain, per time-point) and gastrocnemius LC3 mRNA expression (corrected for GAPDH and normalized to BL6 control) was determined by qRT-PCR. *P<0.05 vs. strain-specific control. †P<0.05 vs. strain-specific HLI d3. **B, C**. LC3II protein abundance was determined in HLI d7 gastrocnemius (Gastroc) by western blotting using GAPDH as a loading control (**B**) and quantified relative to GAPDH and normalized to non-ischemic BL6 controls (**C**). *P<0.05 vs. strain-specific control. **D.** BALB/c mice injected IV with AAVs encoding GFP (N=5), BAG3[Met81] (N=6), or BAG3[Ile81] (N=6) were subjected to modified HLI with collateral vessels left intact, and gastroc LC3 mRNA expression (corrected for GAPDH and normalized to BL6 control) was determined by qRT-PCR. *P<0.05 vs. control. †P<0.05 vs. GFP or BAG3[Met81]. **E, F**. LC3bII protein abundance was determined in Gastroc muscle lysates from BALB/c mice injected IV with AAVs by western blotting using GAPDH as a loading control (**E**) and quantified relative to GAPDH and normalized BL6 controls (**F**). In panel (**E**) all bands are from the same blot and exposure, and the vertical line indicates where the blots were cropped and lanes spliced together for comparison. †P<0.05 vs. GFP or BAG3[Met81]. All data are means ± SEM.

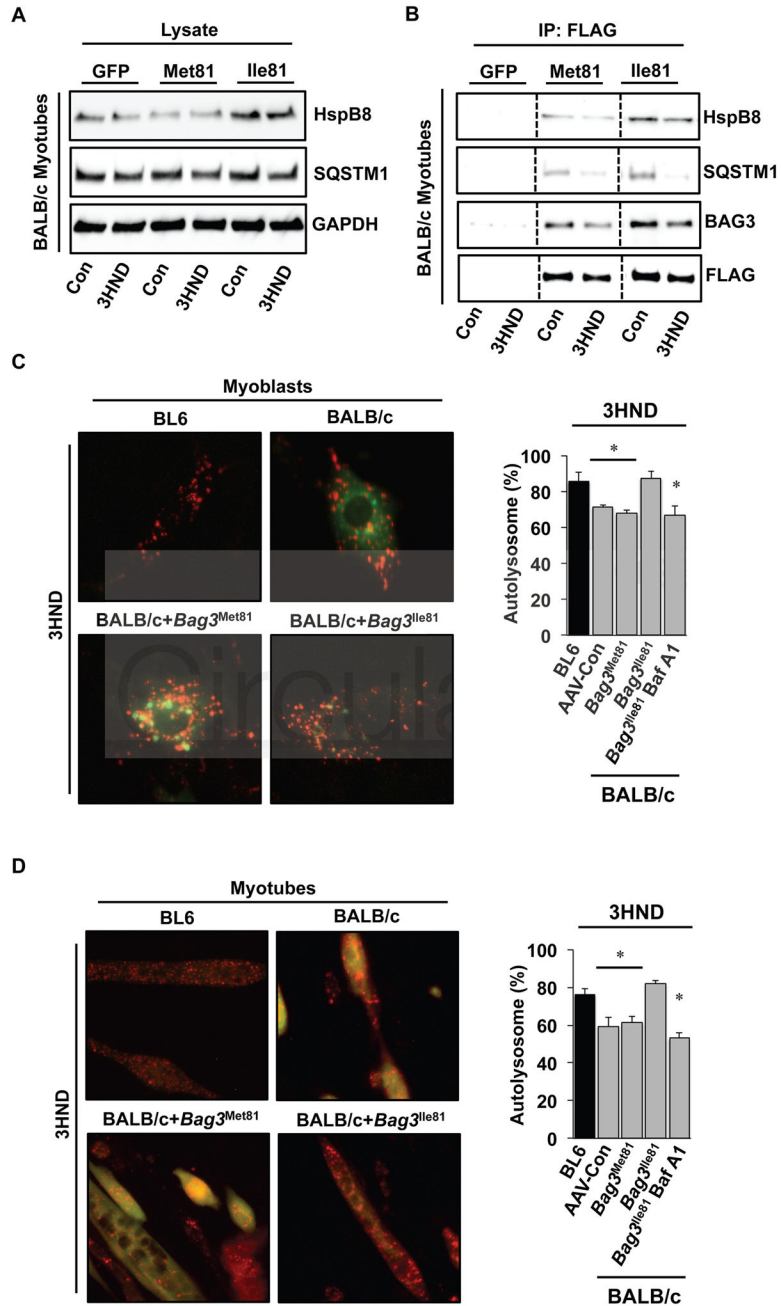**Figure 8. BAG3^{Ile81} differentially binds HspB8 and rescues ischemic autophagic flux in BALB/c muscle cells**

A. BALB/c primary muscle cells were infected with viruses encoding GFP, BAG3^{Met81}, or BAG3^{Ile81} and allowed to differentiate for 96h before experimental ischemia (3HND). Whole cell lysates were immunoblotted for HspB8 and SQSTM1 (p62). **B**. FLAGBAG3 was immunoprecipitated from total cell lysates (**A**) to examine the expression of BAG3 protein and the association of HspB8 and SQSTM1 with exogenously expressed BAG3. All bands in each blot are from the same membrane and exposure time, and the vertical lines indicate where the blots were cropped and lanes spliced together for comparison.

Immunoprecipitations were performed in 3 independent experiments. **C, D.** To examine autophagic flux, BALB/c primary myoblasts (**C**) or myotubes differentiated for 96h (**D**) were infected with an adenovirus expressing membrane-localized red fluorescent protein (mRFP-EGFP-LC3) and adeno-associated viruses (AAV6) encoding a luciferase control, BAG3^{Met81}, or BAG3^{Ile81} then subjected to experimental ischemia (3HND). Bafilomycin A1 (200nM) was used as a positive control. Representative IF images of mRFP-EGFP-LC3 in BALB/c myoblasts (**C**) and myotubes (**D**) are shown (left panels), and the percentage of autolysosomes (mRFP^{+}/eGFP^{-} puncta) were quantified (right panels). *P<0.05 vs. BL6.